

# RE-CONSTRUCTION OF CH<sub>4</sub> EMISSIONS FROM A BIOGAS PLANT – METEOROLOGICAL ASPECTS

Martin Piringer<sup>1</sup>, Marlies Hrad<sup>2</sup>, Sirma Stenzel<sup>1</sup> and Marion Huber-Humer<sup>2</sup>

<sup>1</sup>Department of Environmental Meteorology, Central Institute for Meteorology and Geodynamics, Vienna, Austria

<sup>2</sup>Institute of Waste Management, BOKU-University, Vienna, Austria

**Abstract:** The re-construction of emissions by an inverse dispersion technique depends, among others, on the appropriate meteorological input. For the biogas plant under investigation, it is provided by a 3D ultrasonic anemometer at a representative position at the facility. CH<sub>4</sub> concentration measurements are available for selected days from an Optical Remote Sensing Technique. For the back-calculation of emissions in this complex environment of buildings of different size, tanks and other industrial parts, the Lagrange particle diffusion model LASAT is used. As up to 12 possible sources have been identified, back-calculation is a multi-source problem. First results of source strength identification and a meteorological interpretation are presented.

**Key words:** *Optical Remote Sensing Technique, multi-source reconstruction, ultrasonic anemometer, Lagrange dispersion model, methane, recovery ratio, condition number.*

## INTRODUCTION

Greenhouse gas emissions and methane losses can arise from diverse parts of biogas facilities along the entire process chain of biogas generation and utilization. We try to quantify such emissions and losses in the frame of an on-going research project by combining an Optical Remote Sensing (ORS) technology (OP-TDLS) to detect the spatial and temporal behaviour of the plumes and Lagrange dispersion modelling to re-construct the emissions using an inverse dispersion technique. A pre-requisite of accurate dispersion modelling is the appropriate meteorological input provided by a 3D ultrasonic anemometer at a representative position at the biogas facility under investigation.

First, besides a brief presentation of the experimental set-up, the source identification technique for the re-construction of multiple emissions will be outlined. The re-construction with the Lagrange dispersion model LASAT will then be demonstrated for a biogas plant NW of Vienna where up to 12 possible sources of CH<sub>4</sub> (digestate storage tank, gas tank, gas engine, substrate storage, etc.) have been identified. The plant is made up of various objects (tanks, buildings, etc.) with different sizes and heights which poses a challenge for near-field dispersion modelling. The open path measurements are done for up to 17 different paths across the plant in order to cover all possible emission sources. Based on the measured concentrations along the paths and the meteorological data set, the source strength identification method is tested by first assuming that all sources have equal emission flow rates and second, by more realistic assumptions of emission strengths of each source. As a consequence, the contribution of each individual source to the measured total concentrations will be obtained.

## EXPERIMENTAL SET-UP

As an example, based on a photograph of the biogas plant under consideration, the laser paths (black lines) for the digestate storage tanks together with a picture and the position of the ultrasonic anemometer (red filled circle) are shown in Fig. 1. This arrangement is measured twice a month for several hours in order to evaluate the variability in the short-term emissions. The configuration depicted in Fig. 1 is used to quantify sources  $Q_1$  to  $Q_5$  by selecting the appropriate path depending on the prevailing wind direction and taking the maximum concentration measured along this path. A more detailed description of the measurement technique is given in Hrad et al. (2012).

## SOURCE STRENGTH IDENTIFICATION AND DISPERSION MODEL

Usually, a dispersion model is used to calculate ambient concentrations on the basis of known emissions. In case the emissions are not known, they can also be back-calculated from measured concentrations. The emission rate  $Q$  (mg/s) for a single source is calculated from the measured ambient concentration  $C$ , the unity emission  $Q_0$  and the corresponding ambient concentration  $C_0$  obtained by the Lagrange model LASAT according to the following equation (Flesch et al., 2005; Schaubberger et al., 2011):

$$Q = C (Q_0/C_0) \quad (1)$$

The application of the method for a multi-source problem as in the current case is done with a set of linear equations as described in detail in Flesch et al. (2009) which requires at least as many concentration paths as sources. For two emission rates  $Q_1$  and  $Q_2$  and two receptors  $A$  and  $B$ , the appropriate equation in matrix notation is

$$\begin{bmatrix} (C_{A,1}/Q_1)_{sim} & (C_{A,2}/Q_2)_{sim} \\ (C_{B,1}/Q_1)_{sim} & (C_{B,2}/Q_2)_{sim} \end{bmatrix} \begin{bmatrix} Q_1 \\ Q_2 \end{bmatrix} = \begin{bmatrix} C_A \\ C_B \end{bmatrix} \quad (2)$$

The so-called condition number  $\kappa$  is a measure of “ill-conditioning”, i.e. if the solution is extremely sensitive to changes in the input data (measurements or model estimates), and for the above matrix is given by

$$\kappa = \left\| (C/Q)_{sim} \right\| * \left\| (C/Q)_{sim}^{-1} \right\| \quad (3)$$

According to Flesch et al. (2009), source decomposition is possible if  $10 < \kappa < 20$ ; for the total emission of all sources,  $\kappa < 50$ .

The accuracy of the emission calculations is, as in Flesch et al. (2009), measured as so-called gas recovery ratio  $R$ , definable for each source ( $R_i$ ) as well as for the sum of sources ( $R_{total}$ ) investigated (total recovery ratio). A perfect calculation gives  $R = 1$ . For the current application in which the dispersion model LASAT is used,  $R$  is given by

$$R = Q_{mod}/Q_{fix} \quad (4)$$

where  $Q_{mod}$  is the calculated emission rate via LASAT, while  $Q_{fix}$  is the fixed (assumed) emission. The dispersion model LASAT (Janicke Consulting, 2011; <http://www.janicke.de>) simulates the dispersion and the transport of a representative sample of tracer particles utilizing a random walk process (Lagrange simulation). It computes the transport of passive tracer substances in the lower atmosphere (up to heights of about 2000 m) on a local and regional scale. LASAT includes a mass-consistent diagnostic wind field model which takes into account for enhanced turbulence and re-circulation effects around buildings. The model can use the complete meteorological and turbulence information of a 3D ultrasonic anemometer, including a vertical profile. Especially atmospheric stability is directly deduced from the measured turbulence (Monin-Obukhov length).



Figure 1. Sources, laser paths, picture and location (red dot) of the ultrasonic anemometer at the biogas plant (north orientated)

## RESULTS AND DISCUSSION

The site experiences average wind speeds of about  $3 \text{ ms}^{-1}$ , and the distribution of wind directions and wind speeds during daytime is shown in Figure 2. Winds from South-west are most common and show also a considerable fraction of speeds above  $7 \text{ ms}^{-1}$ . In anti-cyclonic conditions often occurring on the sampling days, easterly winds are quite frequent. Both wind direction segments are favourable for the orientation of the laser paths (Figure 1). Atmospheric stability is determined from the Monin-Obukhov length deduced from the 3D

ultrasonic anemometer. On average, this parameter shows unstable conditions during daytime and stable conditions during night, as expected (not shown).

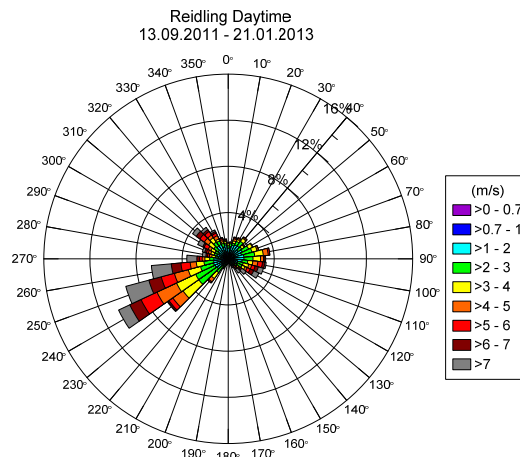


Figure 2. Daytime wind rose measured by the 3D ultrasonic anemometer at the biogas plant.

The re-construction of the emissions of the five sources in Fig. 1 is tried for six selected days (Table 1), assuming emission rates of  $3\text{gs}^{-1}$  for sources  $Q_2$ ,  $Q_3$  and  $Q_5$ , and  $0,5\text{gs}^{-1}$  for  $Q_1$  and  $Q_4$ . These emissions rates have been arbitrarily selected, giving a greater weighing to the sources  $Q_2$ ,  $Q_3$  and  $Q_5$ , which represent open digestate storage tanks. In contrast, the weaker sources  $Q_1$  and  $Q_4$  constitute of closed tanks of liquid manure, which have only small openings for the stirrer. The recovery rates for each individual source and each time step for January 24, 2012 are shown in Fig. 3. Negative values of  $R$  imply that an emission sink that absorbs  $\text{CH}_4$  within the area best explains the observations (Flesch et al., 2009). Sources  $Q_3$  and  $Q_5$  are recovered with the lowest scatter, followed by  $Q_2$ . The weak sources  $Q_1$  and  $Q_4$  are less well recovered; there is a large scatter of the recovery ratios over time between five times over-estimation and a sink up to twice as large as the actual emission. On this day, the main wind direction was from WNW with an average wind speed of  $5,5\text{ms}^{-1}$ ; atmospheric stability could be classified as neutral throughout the day. The wind was thus blowing relatively steady “from left to right” through the biogas plant in the course of the several hours of calculations, and a meteorological reason for the poorer identification of sources 1 and 4 compared to the others cannot be deduced easily. It is evident that the larger sources dominate the dispersion and are thus better identified in the matrix algorithm.

Table 1: Short characterization of the days of the experiment

1. 23.01.2012: WSW-Wind  $7\text{ms}^{-1}$ , stability: neutral (all storage tanks filled); digestate sample of  $Q_3$
2. 24.01.2012: WNW-Wind  $5,5\text{ms}^{-1}$ , stability: neutral (all storage tanks filled)
3. 08.02.2012: NE-SE-Wind  $2,5\text{ms}^{-1}$ , stability: variable (all storage tanks filled)
4. 06.03.2012: NE-E-Wind  $2,5\text{ms}^{-1}$ , stability: unstable (storage tanks partly filled since 15.02); digestate sample of  $Q_3$
5. 10.07.2012: SE-Wind  $2\text{ms}^{-1}$ , stability: unstable (only  $Q_3$  filled); digestate sample of  $Q_3$
6. 16.08.2012: SW-Wind  $3\text{ms}^{-1}$ , stability: neutral (only  $Q_3$  filled); digestate sample of  $Q_3$

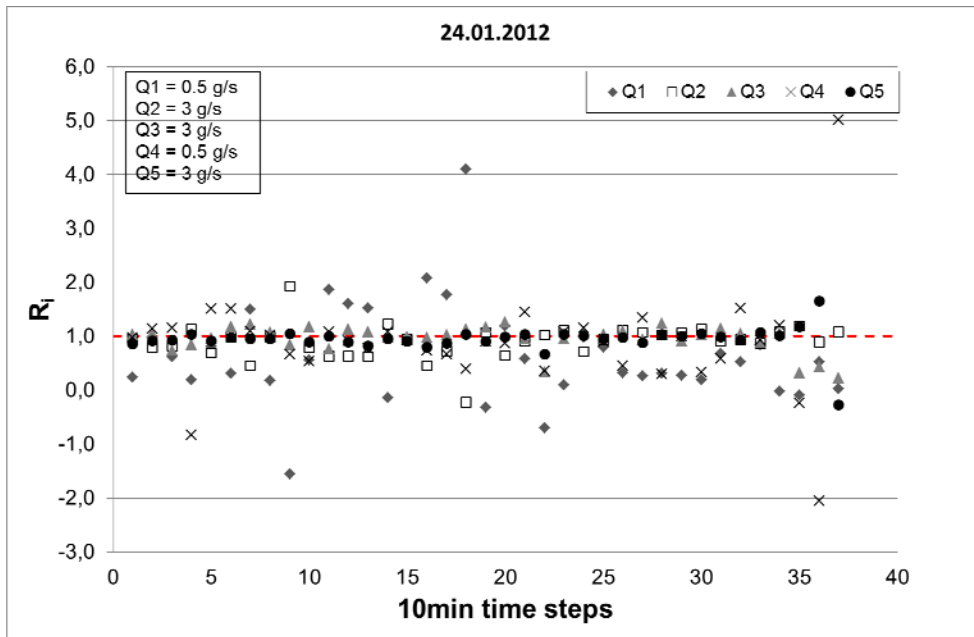


Figure 3: Time series of recovery ratios  $R_i$  for five sources on January 24, 2012

For all days of the experiment, we find a weak dependence of the total recovery ratio on the condition number (Fig. 4).  $R_{total}$  mostly varies between two times over-estimation and 70 % under-estimation, with a lot more cases of slight under-estimation on all experiment days. The few outliers are found for condition numbers well above 20. The outliers are mainly found on days 4 and 5 which were the two days with unstable conditions and weak winds; in such conditions, vertical plume propagation and plume meandering is strongest, leading to a large variability of ground concentrations in space and time. The three days with neutral stratification show mostly low condition numbers, even with weak winds as on day 6. In these cases, vertical turbulence and thus the resulting special plume effects (mentioned above) are reduced. Of all meteorological parameters investigated, the dependence of the condition number on wind speed is strongest: large condition numbers indicating uncertainty in recovering the sources are found for wind speeds below  $4 \text{ ms}^{-1}$  only (Fig. 5). The latter are mainly associated with experimental days 3 to 5 on which wind speeds were lowest on average.

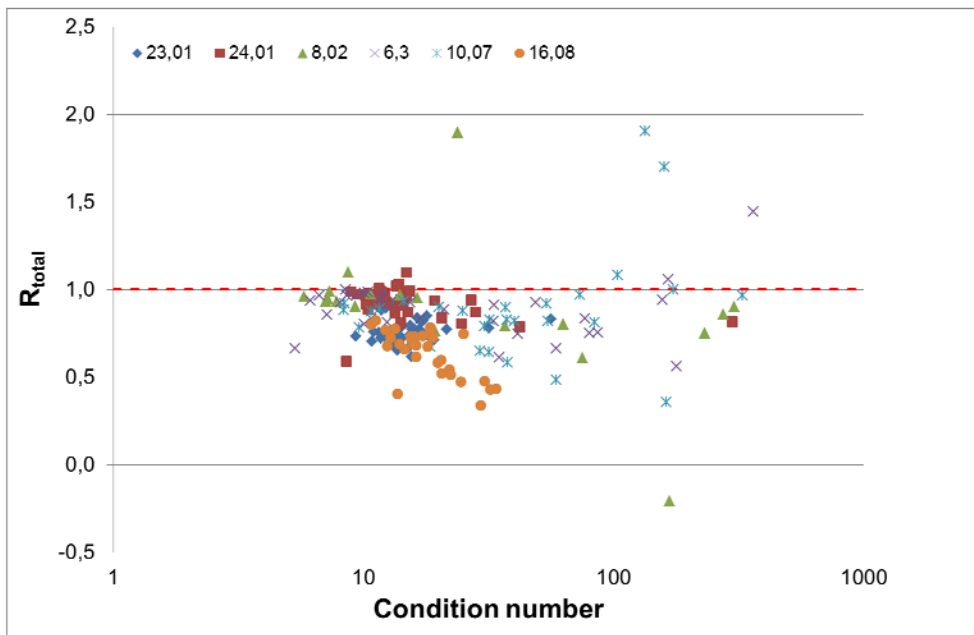


Figure 4: Dependence of the total recovery ratio  $R_{total}$  for each experimental day on the condition number  $\kappa$

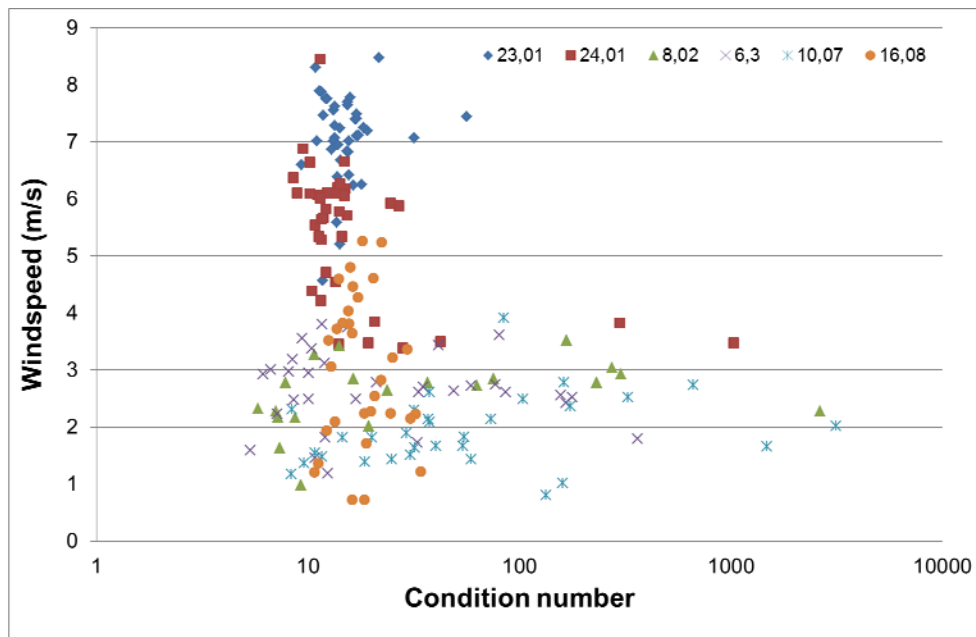


Figure 5: Dependence of the condition number  $\kappa$  on wind speed for all experimental days

## SUMMARY AND CONCLUSIONS

For a biogas plant NW of Vienna, Austria, CH<sub>4</sub> source identification was undertaken by a combination of an Optical Remote Sensing Technique and a Lagrangian dispersion model resolving the complex building structure and incorporating different kinds of sources. For six experimental days with different meteorological conditions (Table 1), the individual and total recovery ratios were calculated and interpreted with respect to the condition number and the wind speed. Source strength identification works best for higher emissions (Fig. 3), larger wind speeds and neutral atmospheric stability (Figs. 4 and 5).

The algorithm of source strength identification is based on investigations by Flesch et al. (2009) and was applied here for real-world case studies. The results are satisfactory for the six days selected for the investigation which are characterized by a large variety of wind directions, wind speeds and stability conditions.

## REFERENCES

- Flesch, Th. K., L. A. Harper, R. I. Desjardins, Z. Gao, Z. and B. P. Crenna, 2009: Multi-source emission determination using an inverse-dispersion technique. *Boundary-Layer Meteorol.*, **132**, 11-30.
- Flesch, Th. K., J. D. Wilson, L. A. Harper, B. P. Crenna, 2005: Estimating gas emissions from a farm with an inverse-dispersion technique. *Atmospheric Environment*, **39**, 4863-4874.
- Hrad, M., M. Huber-Humer, M. Piringer, 2012: Development of a quantification tool for greenhouse gas monitoring using OP-TDLS systems. *Global Waste Management Symposium*, 30. Sept. – 3. Oct. 2012, Phoenix, USA.
- Janicke Consulting, 2011: Dispersion Model LASAT Version 3.2 Reference book.
- Schauberger, G., M. Piringer, W. Knauder, E. Petz, 2011: Odour emissions from a waste treatment plant using an inverse dispersion technique. *Atmospheric Environment*, **45**, 1639-1647.